

1 **Impacts of non-canonical El Niño patterns on Atlantic hurricane activity**

2  
3  
4  
5  
6  
7  
8 Sarah Larson<sup>1</sup>, Sang-Ki Lee<sup>2,3</sup>, Chunzai Wang<sup>3</sup>, Eui-Seok Chung<sup>1</sup>, and David Enfield<sup>2,3</sup>

9 <sup>1</sup>Rosenstiel School of Marine and Atmospheric Science, University of Miami, Miami FL

10 <sup>2</sup>Cooperative Institute for Marine and Atmospheric Studies, University of Miami, Miami FL

11 <sup>3</sup>Atlantic Oceanographic and Meteorological Laboratory, NOAA, Miami FL

12  
13  
14  
15  
16  
17  
18 Revision to Geophysical Research Letters

19 May 2012

20  
21  
22 Corresponding author address: Dr. Sang-Ki Lee, NOAA/AOML, 4301 Rickenbacker Causeway,  
23 Miami, FL 33149, USA. E-mail: [Sang-Ki.Lee@noaa.gov](mailto:Sang-Ki.Lee@noaa.gov).

24  
25  
26  
27  
28  
29  
30  
31  
32  
33  
34  
35  
36  
37  
38  
39  
40  
41  
42  
43  
44  
45  
46

## Abstract

The impact of non-canonical El Niño patterns, typically characterized by warmer than normal sea surface temperatures (SSTs) in the central tropical Pacific, on Atlantic tropical cyclone (TC) is explored by using composites of key Atlantic TC indices and tropospheric vertical wind shear over the Atlantic main development region (MDR). The highlight of our major findings is that, while the canonical El Niño pattern has a strong suppressing influence on Atlantic TC activity, non-canonical El Niño patterns considered in this study, namely central Pacific warming, El Niño Modoki, positive phase Trans-Niño, and positive phase Pacific meridional mode, all have insubstantial impact on Atlantic TC activity. This result becomes more conclusive when the impact of MDR SST is removed from the Atlantic TC indices and MDR wind shear by using the method of linear regression. Further analysis suggests that the tropical Pacific SST anomalies associated with the non-canonical El Niño patterns are not strong enough to cause a substantial warming of the tropical troposphere in the Atlantic region, which is the key factor that increases the wind shear and atmospheric static stability over the MDR. During the recent decades, the non-canonical El Niños have been more frequent while the canonical El Niño has been less frequent. If such a trend continues in the future, it is expected that the suppressing effect of El Niño on Atlantic TC activity will diminish and thus the MDR SST will play a more important role in controlling Atlantic TC activity in the coming decades.

47 **1. Introduction**

48 Warm sea surface temperature (SST) anomalies in the tropical Pacific induce a global  
49 average warming of the tropical troposphere, via a fast tropical teleconnection mechanism (i.e.,  
50 Kelvin waves), and thus increase the meridional tropospheric temperature gradient within and  
51 across the edge of the tropics [e.g., Horel and Wallace 1981; Yulaeva and Wallace 1994; Chiang  
52 and Sobel 2002]. This, in turn, directly increases the vertical wind shear over the Atlantic main  
53 development region (MDR, 10°N – 20°N and 85°W – 15°W), via the thermal wind relationship.  
54 Additionally, the teleconnected tropospheric warming over the tropical Atlantic also tends to  
55 increase atmospheric static stability and thus causes anomalous diabatic cooling over the MDR  
56 [e.g., Tang and Neelin 2004; Lee et al. 2011]. This, in turn, may force the formation of a  
57 stationary baroclinic Rossby wave northwest of the MDR, consistent with Gill’s simple model of  
58 tropical atmospheric circulations, to further increase the MDR wind shear [e.g., Lee et al. 2011].  
59 El Niño events are thus associated with decreased tropical cyclone (TC) activity in the Atlantic  
60 basin especially in the deep tropics as a result of increased wind shear and atmospheric static  
61 stability over the MDR [e.g., Gray 1984; Goldenberg and Shapiro 1997; Kossin et al. 2010;  
62 Klotzbach 2011]. Other environmental factors such as reduced relative humidity also contribute  
63 to decreased Atlantic TC activity during El Niño years, as shown in Carmargo et al. [2007] using  
64 a TC genesis index.

65 The canonical El Niño is characterized by warmer than normal SSTs in the eastern tropical  
66 Pacific Ocean. However, El Niño comes in many different flavors – every El Niño event has a  
67 somewhat different and distinct character [Trenberth and Stepaniak 2001]. Recently, a newly  
68 identified pattern of central equatorial Pacific warming event (non-canonical El Niño hereafter)  
69 has received attention due to its increasing frequency in recent decades and its potential link to

70 the influence of anthropogenic global warming [Yeh et al. 2009; Lee and McPhaden 2010]. This  
71 non-canonical El Niño is referred to as central Pacific El Niño, El Niño Modoki, warm pool El  
72 Niño, Pacific meridional mode and Trans-Niño in the literature [e.g., Yeh et al. 2009; Ashok et  
73 al. 2007; Kao and Yu 2009; Kug et al. 2009; Chiang and Vimont 2004; Trenberth and Stepaniak  
74 2001]. It differs from the canonical El Niño in that its warm equatorial SST anomalies are  
75 concentrated in the central Pacific with cool SST anomalies flanked in a horseshoe pattern to the  
76 east and west [Ashok et al. 2007]. While the canonical El Niño is historically defined as warm  
77 SST anomalies in the Niño-3 region (NINO3; 5°S - 5°N, 150°W - 90°W) or Niño-3.4 region  
78 (NINO3.4; 5°S - 5°N, 170°W - 120°W), several different definitions of the non-canonical El  
79 Niño have been referenced in recent literature – central Pacific warming [CPW; Yeh et al. 2009],  
80 El Niño Modoki index [EMI; Ashok et al. 2007], Pacific meridional mode [PMM, Chiang and  
81 Vimont 2004] and Trans-Niño index [TNI, Trenberth and Stepaniak 2001]. These definitions  
82 were derived to describe the same anomalous central Pacific warming pattern that is captured by  
83 the 2nd mode of the empirical orthogonal function analysis of monthly tropical Pacific SST  
84 anomalies [EOF2, Trenberth and Stepaniak 2001; Ashok et al. 2007].

85 Given a strong dependence of overall Atlantic TC activity on the equatorial Pacific SST  
86 anomalies associated with El Niño, there is a clear need for understanding how the response of  
87 Atlantic TC activity to non-canonical El Niño differs from that to canonical El Niño. A recent  
88 study by Kim et al. [2009] suggested that CPW events are associated with a greater-than-average  
89 frequency of tropical storms and increasing landfall potential along the Gulf of Mexico coast and  
90 Central America. However, Lee et al. [2010] performed an independent data analysis to point out  
91 that such conclusion could be premature because Kim et al. [2009] did not remove in their  
92 analysis the local impact of MDR SST, which is as important as the remote impact of tropical

93 Pacific SSTs as shown overwhelmingly in earlier studies [e.g., Knaff 1997; Knight et al. 2006;  
94 Wang et al. 2006; Zhang and Delworth 2006; Vimont and Kossin 2007; Kossin and Vimont  
95 2007; Saunders and Lea 2008].

96 Both Kim et al. [2009] and Lee et al. [2010] considered only a small number of CPW events  
97 to arrive at the contradicting conclusions. Therefore, here, we further attempt to isolate and  
98 quantify the impact of non-canonical El Niño on Atlantic TC by using composites of SST, VWS  
99 and key Atlantic TC indices for various non-canonical El Niño definitions, i.e, CPW, EMI, TNI  
100 and PMM. One of the key points in our analyses is that, in order to isolate the impact of non-  
101 canonical El Niño, the influence of MDR SST is objectively removed from the Atlantic TC  
102 indices and MDR wind shear prior to making the composites by using the method of linear  
103 regression.

104

## 105 **2. Data**

106 The SST dataset used in this study is the NOAA Extended Reconstructed Sea Surface  
107 Temperature version 3 [ERSST3; Smith et al. 2008] for the Atlantic hurricane season of June to  
108 November (JJASON) from the period of 1950 - 2010. The NCEP-NCAR Reanalysis-1 data for  
109 the same season and period is used to compute the wind shear and geopotential thickness  
110 between 200 and 850 hPa [Kalnay et al. 1996]. The hurricane reanalysis database (HURDAT)  
111 from the National Hurricane Center for the same period is used to obtain various Atlantic TC  
112 indices.

113 As discussed earlier, in order to isolate the impact of non-canonical El Niño patterns, the  
114 influence of MDR SST is removed from the Atlantic TC indices and wind shear by using the

115 method of linear regression. For example, the modified MDR vertical wind shear (VWS) can be  
116 obtained by

$$117 \quad \text{MDR VWS (modified)} = \text{MDR VWS} - a \times \text{MDR SSTA}, \quad (1)$$

118 where  $a$  ( $= -1.96 \text{ m s}^{-1} \text{ }^\circ\text{C}^{-1}$ ) is the regression coefficient of anomalous MDR SST onto the MDR  
119 wind shear (see Figure S1). All of our analyses in section 4 are performed both with and without  
120 this approach.

121

### 122 **3. Indices for Non-canonical El Niño Patterns**

123 As pointed out by Ashok et al. [2007], the EOF2 of monthly tropical Pacific SST anomalies  
124 captures the distinct SST anomaly structure characteristic of the non-canonical El Niño. Various  
125 indices, such as CPW, EMI, TNI, and PMM have been suggested and used to define this same  
126 phenomenon. Currently, there is no consensus on how to classify the non-canonical El Niño.  
127 Hence, CPW, EMI, TNI and PMM are all reproduced for this study as described below. The  
128 referenced regions of SST anomalies are depicted in Figure S2 (and in Figure 1).

129 Ashok et al. [2007] proposed EMI to determine non-canonical El Niño years. EMI is  
130 calculated using the following equation:

$$131 \quad \text{EMI} = [\text{SSTA(A)} - 0.5 \times \text{SSTA(B)} - 0.5 \times \text{SSTA(C)}], \quad (2)$$

132 where SSTA(A) is the SST anomalies averaged over a box region for  $10^\circ\text{S} - 10^\circ\text{N}$  and  $165^\circ\text{E} -$   
133  $140^\circ\text{W}$ , SSTA(B) is for  $15^\circ\text{S} - 5^\circ\text{N}$  and  $110^\circ\text{W} - 70^\circ\text{W}$ , and SSTA(C) is for  $10^\circ\text{S} - 20^\circ\text{N}$  and  
134  $125^\circ\text{E} - 145^\circ\text{E}$ . In this study, the index is normalized ([ ] represents normalization) by the  
135 standard deviation of the EMI time series.

136 Yeh et al. [2009] defined non-canonical El Niño years by establishing a set of criteria for  
137 what is called CPW. A CPW year occurs when warm SST anomaly in the Niño-4 region (NINO4;

138 5°S - 5°N, 160°E - 150°W) exceeds that of the Niño-3 region [Yeh et al. 2009]. Note that CPW is  
139 not an index but rather criteria for handpicking non-canonical El Niño years, thus a CPW time  
140 series cannot be computed. CPW years are defined as those years in which NINO4 is greater than  
141 NINO3, while NINO4 is positive.

142 Chiang and Vimont [2004] proposed PMM to describe an anomalous SST gradient across the  
143 mean latitude of the intertropical convergence zone (ITCZ) coupled to an anomalous  
144 displacement of the ITCZ toward the warmer region. PMM is calculated in this study using the  
145 following equation:

$$146 \quad \text{PMM} = [[\text{ENP}] - [\text{NINO1+2}]], \quad (3)$$

147 where ENP (eastern North Pacific) is the SST anomaly averaged over a box region for 10°N -  
148 30°N and 140°E - 110°W, and NINO1+2 is the SST anomaly averaged over the Niño-1+2 region  
149 (10°S - 0°N, 90°W -80°W). In this study, the index is normalized by the standard deviation of the  
150 PMM time series.

151 Trenberth and Stepaniak [2001] suggested that an optimal characterization of both the  
152 distinct character and the evolution of each El Niño and La Niña event requires a so-called TNI  
153 in addition to the conventional SST anomalies in the Niño-3.4 region. TNI is computed by taking  
154 the difference between the normalized SST anomalies averaged in the Niño-1+2 and Niño-4  
155 regions then further normalizing the resulting time series to have unit standard deviation. By  
156 normalizing the Niño-1+2 and Niño-4 SST anomaly terms prior to subtraction, neither region's  
157 SST anomaly can dominate the overall index. This is necessary because the magnitude of the  
158 equatorial eastern Pacific SST anomaly is usually larger than equatorial central Pacific SST  
159 anomaly. The resulting TNI is SST anomaly difference between the Niño-1+2 and Niño-4  
160 regions. Note that Trenberth and Stepaniak [2001] calculate TNI by subtracting Niño-4 SST

161 anomalies from Niño-1+2 SST anomalies so that a positive index corresponds to a cold central  
162 equatorial Pacific event. Here, in order for a positive TNI to correspond to a warmer than normal  
163 SST anomalies in the central tropical Pacific, the normalized Niño-1+2 SST anomalies are  
164 subtracted from the normalized Niño-4 SST anomalies in this study. Therefore, the equation for  
165 TNI is given by

$$166 \quad \text{TNI} = [[\text{NINO4}] - [\text{NINO1+2}]], \quad (4)$$

167 where [ ] represents that the variable is normalized.

168 To represent each non-canonical El Niño definition, composites of the eight strongest  
169 positive (warm) phase years, during which NINO4 is also positive, are created for CPW, EMI,  
170 TNI and PMM. An additional criterion of NINO4 > 0 is required to eliminate years in which  
171 other regions' cold SST anomalies account for the positive index. For example, when calculating  
172 TNI, if NINO4 is 0 and NINO1+2 is negative, then TNI > 0. However, this is not a central  
173 tropical Pacific warming event but rather an eastern tropical Pacific cooling event. Therefore,  
174 including the criterion of NINO4 > 0 in selecting non-canonical El Niño years ensures that these  
175 types of years are discarded. NINO3 is also computed for the period 1950 – 2010 to create the  
176 composite of the eight strongest canonical El Niño years. Hereafter, NINO3 is also referred to as  
177 eastern Pacific warming (EPW). Note that each of these indices is first averaged for JJASON,  
178 and then is used in selecting the eight strongest positive phase years.

179 Figure S3 displays the time series of EMI, TNI, PMM and EPW for JJASON during the  
180 period 1950 – 2010. EOF2 contains a strong low frequency signal, and is largely positive (i.e.,  
181 warmer than normal in the central Pacific) during 1950-1970 and negative (i.e., colder than  
182 normal in the central Pacific) during 1997-2010 (not shown). EMI, TNI and PMM show more  
183 variability at the short time scales than EOF2. Overall, EMI and TNI agree in term of phase with

184 the correlation coefficient of 0.86 (see Table S1). Similarly, TNI and PMM are significantly  
185 correlated with the correlation coefficient of 0.70, whereas EMI and EPW are poorly correlated  
186 with the correlation coefficient of 0.17.

187

#### 188 **4. Non-canonical El Niño Patterns and Atlantic TC Activity**

189 To quantify the impact of non-canonical El Niño on Atlantic TC activity, the number of  
190 tropical storms (TS), hurricanes (HR), major hurricanes (MH, categories 3-5), accumulated  
191 cyclone energy (ACE), number of United States landfalling hurricanes (USL), and the MDR  
192 wind shear for JJASON are averaged for each index's eight-year composite before and after  
193 removing the effect of Atlantic MDR SST (Table 1). For reference, the Atlantic TC indices and  
194 MDR wind shear for each of the eight strongest positive phase years for CPW, EMI, TNI, PMM,  
195 and EPW are shown in Table S2, S3, S4, S5, and S6, respectively.

196 It is clear from Table 1 that only EPW shows all Atlantic TC indices (i.e., TS, HR, MH, ACE  
197 and USL) decreased and the MDR wind shear increased at the 90% significance level. Removing  
198 the effect of the Atlantic MDR SST has very minor impact (parenthesized values). In CPW and  
199 EMI, some Atlantic TC indices are decreased and the MDR wind shear is slightly increased  
200 before and after the Atlantic MDR SST impact is removed. However, these changes are too small  
201 to be statistically significant at the 90% level. In TNI, on the other hand, some Atlantic TC  
202 indices (i.e., TS, HR and ACE) are increased and the MDR wind shear is decreased before the  
203 Atlantic MDR SST impact is removed (non-parenthesized value). After the Atlantic MDR SST  
204 impact is removed (parenthesized value), however, all Atlantic TC indices and the MDR wind  
205 shear recover their climatological values. In PMM, all Atlantic TC indices are virtually  
206 indistinguishable from their climatological values. Removing the effect of the Atlantic MDR SST

207 has no impact in this case (parenthesized values).

208 In summary, in agreement with earlier studies [e.g., Gray 1984; Goldenberg and Shapiro  
209 1997; Kossin et al. 2010; Klotzbach 2011], we find consistent evidence that the canonical El  
210 Niño suppresses Atlantic TC activity due to a large increase of the MDR wind shear. Some non-  
211 canonical El Niño patterns (CPW and EMI) also tend to slightly suppress Atlantic TC activity  
212 due to a weak-to-moderate increase of the MDR wind shear. However, their impact is  
213 insubstantial in comparison to that of the canonical El Niño. Therefore, here we do not find any  
214 evidence that links any of the four non-canonical El Niño patterns to Atlantic TC activity. This  
215 conclusion is also valid if Atlantic TC activity during the most active season of August-October  
216 (ASO) is considered (see Table S7).

217

## 218 **5. Comparison with Earlier Studies**

219 Kim et al. [2009] and Lee et al. [2010] considered only five strongest CPW years, whereas  
220 this study uses eight strongest positive phase years for CPW (as well as for EMI, TNI and PMM).  
221 To test if our main conclusion is affected by the sample size, Table 1 is reproduced by using only  
222 the five strong positive phase years for each ENSO index (Table S8). As shown in the new table,  
223 the Atlantic TC indices and MDR wind shear are affected significantly (at the 90% significance  
224 level) only by the canonical El Niño (EPW), consistent with our main conclusion.

225 It is also worthwhile to point out that Kim et al. [2009] identified the five strongest CPW  
226 years (1969, 1991, 1994, 2002, and 2004) based on linearly detrended tropical Pacific SSTs  
227 averaged for ASO. In this study, tropical Pacific SSTs (as well as tropical Atlantic SSTs) and  
228 Atlantic TC indices are not detrended and they are averaged for JJASON. Due to these  
229 differences, 1969 and 1991 were identified as CPW years in Kim et al. [2009], but they are not

230 included in the list of eight strongest CPW years (see Table S2). Interestingly, 1991 is identified  
231 as a canonical El Niño year (Table S6). However, if tropical Pacific SSTs are averaged for ASO,  
232 1991 is indeed identified as a strong CPW year. 1991 was a year of below normal Atlantic TC  
233 activity (see Table S6 and S9). 1969, on the other hand, was a year of much increased Atlantic  
234 TC activity (Table S9). However, ASO of 1969 should be considered as a weak-to-moderate  
235 canonical El Niño season because NINO3 was only 0.63°C and greater than NINO4 (0.58°C).

236

## 237 **6. Tropical Teleconnections Induced by Non-canonical El Niño Patterns**

238 Two key differences between the four non-canonical El Niño patterns and the canonical El  
239 Niño pattern are seen in the tropical Pacific SST anomaly distributions for JJASON (Figure 1).  
240 First, the maximum (warm) SST anomalies for the four non-canonical El Niño patterns are  
241 located in either the central tropical Pacific (EMI) or near the dateline (CPW, TNI and PMM),  
242 whereas those for the canonical El Niño are in the eastern tropical Pacific. But, more importantly,  
243 the amplitude of tropical Pacific SST anomalies associated with the non-canonical El Niño  
244 patterns is much weaker than that of the canonical El Niño. Consequently, the tropical  
245 tropospheric warming associated with the four non-canonical El Niño patterns is relatively weak  
246 and largely confined in the tropical Pacific region (Figure 2a – d). EOF2 correlation map of  
247 temperature anomalies at 500 hPa shows a consistent result (see Figure 7 in Trenberth and Smith  
248 2009). In contrast, the tropical tropospheric warming associated with the canonical El Niño is  
249 much stronger, and its teleconnection to the tropical Atlantic region is clearly visible (Figure 2e).  
250 Therefore, we can conclude that the tropical Pacific SST anomalies associated with the non-  
251 canonical El Niño patterns are not strong enough to cause a substantial warming of the tropical  
252 troposphere in the Atlantic region, which is the key factor that increases the meridional

253 tropospheric temperature gradient and atmospheric static stability over the MDR. Note that the  
254 meridional tropospheric temperature gradient over the tropical Atlantic has a direct influence on  
255 the MDR VWS via the thermal wind relationship. The atmospheric static stability and associated  
256 anomalous diabatic heating (or cooling) over the MDR also influence the MDR wind shear via  
257 the formation of a stationary baroclinic Rossby wave northwest of the MDR [e.g., Lee et al.  
258 2011]. Therefore, consistent with the lack of teleconnected tropospheric warming over the  
259 tropical Atlantic in Figure 2a – d, the MDR wind shear anomalies for CPW, EMI, TNI and PMM  
260 are either neutral or only slightly increased (Figure 3a - d).

261

## 262 **7. Discussions**

263 The highlight of our major findings is that some non-canonical El Niño patterns tend to  
264 slightly suppress Atlantic TC activity due to a weak-to-moderate increase of the MDR VWS.  
265 However, the overall impact of non-canonical El Niños is very small compared to that of the  
266 canonical El Niño. This result becomes more conclusive when the effect of MDR SST is  
267 removed from the Atlantic TC indices and MDR wind shear.

268 Recent studies reported that, during the recent decades, the non-canonical El Niños have  
269 been more frequent while the canonical El Niño has been less frequent [Yeh et al. 2009; Lee and  
270 McPhaden 2010]. Yeh et al. [2009] suggested that such trend may continue in the future due to  
271 anthropogenic greenhouse effect on the tropical Pacific thermocline. If this is indeed the case, an  
272 important implication is that the suppressing effect of El Niño on Atlantic TC activity may  
273 diminish and thus the MDR SST may play a more important role in controlling Atlantic TC  
274 activity in the coming decades.

275

276 **Acknowledgments.** We wish to thank Jay Harris and Hailong Liu for their assistance in data  
277 acquisition and processing, and two anonymous reviewers and Greg Foltz for helpful comments  
278 and suggestions. This work was supported by the NOAA Ernest F. Hollings undergraduate  
279 scholarship program, and grants from the NOAA's Climate Program Office and the National  
280 Science Foundation.

281

## 282 **References**

283 Ashok, K., S. Behera, A. S. Rao, H. Y. Weng, T. Yamagata, 2007: El Niño Modoki and its  
284 possible teleconnection, *J. Geophys. Res.*, 112, C1107, doi:10.1029/2006JC003798.

285 Camargo, S. J., K. A. Emanuel and A. H. Sobel, 2007: Use of a genesis potential index to  
286 diagnose ENSO effects on tropical cyclone genesis. *J. Climate*, 20, 4819-4834.

287 Chiang, J. C. H., and A. H. Sobel, 2002: Tropical tropospheric temperature variations caused by  
288 ENSO and their influence on the remote tropical climate. *J. Climate*, 15, 2616–2631.

289 Chiang, J. C. H., D. J. Vimont, 2004: Analogous Pacific and Atlantic meridional modes of  
290 tropical atmosphere–ocean variability. *J. Climate*, 17, 4143–4158.

291 Goldenberg, S. B. and L. J. Shapiro, 1996: Physical mechanisms for the association of El Niño  
292 and West African rainfall with Atlantic major hurricane activity, *J. Climate*, 9, 1169-1187.

293 Gray, W. M., 1984: Atlantic seasonal hurricane frequency. Part I: El Niño and 30 mb Quasi-  
294 Biennial Oscillation influences. *Mon. Wea. Rev.*, 112, 1649-1668.

295 Horel, J. D., and J. M. Wallace, 1981: Planetary-scale atmospheric phenomena associated with  
296 the Southern Oscillation. *Mon. Wea. Rev.*, 109, 813–829.

297 Kalnay et al., 1996: The NCEP/NCAR 40-year reanalysis project, *Bull. Amer. Meteor. Soc.*, 77,  
298 437-470.

299 Kao, H.-Y. and J.-Y. Yu, 2009: Contrasting eastern-Pacific and central-Pacific types of ENSO. *J.*  
300 *Climate*, 22, 615-632.

301 Kim, H.-M., P. J. Webster, J. A. Curry, 2009: Impact of shifting patterns of Pacific Ocean  
302 warming on North Atlantic tropical cyclones, *Science*, 325, 77-80.

303 Klotzbach, P. J., 2011: El Niño–Southern Oscillation’s Impact on Atlantic Basin Hurricanes and  
304 U.S. Landfalls. *J. Climate*, 24, 1252–1263. doi: <http://dx.doi.org/10.1175/2010JCLI3799.1>.

305 Kossin, J. P., and D. J. Vimont, 2007: A more general framework for understanding Atlantic  
306 hurricane variability and trends. *Bull. Amer. Meteor. Soc.*, 88, 1767–1781.

307 Kossin, J. P., S. J. Camargo, and M. Sitkowski, 2010: Climate modulation of North Atlantic  
308 hurricane tracks. *J. Climate*, 23, 3057-3076.

309 Knaff, J. A., 1997: Implications of summertime sea level pressure anomalies in the tropical  
310 Atlantic region. *J. Climate*, 10, 789–804.

311 Knight, J. R., C. K. Folland, and A. A. Scaife, 2006: Climate impacts of the Atlantic  
312 multidecadal oscillation. *Geophys. Res. Lett.*, 33, L17706, doi:10.1029/2006GL026242.

313 Kug, J.-S., F.-F. Jin, S.-I. An, 2009: Two types of El Niño events: cold tongue El Niño and warm  
314 pool El Niño. *J. Climate*, 22, 1499–1515.

315 Lee, S.-K., C. Wang and D. B. Enfield, 2010: On the impact of central Pacific warming events  
316 on Atlantic tropical storm activity. *Geophys. Res. Lett.*, 37, L17702,  
317 doi:10.1029/2010GL044459.

318 Lee, S.-K., D. B. Enfield and C. Wang, 2011: Future impact of differential inter-basin ocean  
319 warming on Atlantic hurricanes. *J. Climate*, 24, 1264-1275.

320 Lee, T., and M. J. McPhaden, 2010: Increasing intensity of El Niño in the central-equatorial  
321 Pacific, *Geophys. Res. Lett.*, 37, L14603, doi:10.1029/2010GL044007.

322 Saunders, M. A., and A. S. Lea, 2008: Large contribution of sea surface warming to recent  
323 increase in Atlantic hurricane activity. *Nature*, 451, 557–560.

324 Smith, T. M., R. W. Reynolds, T. C. Peterson, and J. Lawrimore, 2008: Improvements to  
325 NOAA's historical merged land-ocean surface temperature analysis (1880-2006), *J. Climate*,  
326 21, 2283-2296.

327 Tang, B. H. and J. D. Neelin, 2004: ENSO Influence on Atlantic Hurricanes via Tropospheric  
328 Warming. *Geophys. Res. Lett.*, 31, L24204, doi:10.1029/2004GL021072.

329 Trenberth, K. E., and D. P. Stepaniak, 2001: Indices of El Niño Evolution, *J. Climate*, 14, 1697-  
330 1701.

331 Trenberth, K. E., and L. Smith, 2009: Variations in the three dimensional structure of the  
332 atmospheric circulation with different flavors of El Niño. *J. Climate*, 22, No. 11, 2978-2991,  
333 doi: 10.1175/2008JCLI2691.1.

334 Vimont, D. J., and J. P. Kossin, 2007: The Atlantic meridional mode and hurricane activity.  
335 *Geophys. Res. Lett.*, 34, L07709, doi:10.1029/2007GL029683.

336 Wang, C., D. B. Enfield, S.-K. Lee, and C. W. Landsea, 2006: Influences of Atlantic warmpool  
337 on Western Hemisphere summer rainfall and Atlantic hurricanes. *J. Climate*, 19, 3011–3028.

338 Yeh, S.-W., J.-S. Kug, B. Dewitte, M.- H. Kwon, B. Kirtman, and F.-F. Jin, 2009: El Niño in a  
339 changing climate, *Nature*, 461, 511-514.

340 Yulaeva, E., and J. M. Wallace, 1994: The signature of ENSO in global temperature and  
341 precipitation fields derived from the microwave sounding unit. *J. Climate*, 7, 1719–1736.

342 Zhang, R., and T. L. Delworth, 2006: Impact of Atlantic multidecadal oscillations on India/Sahel  
343 rainfall and Atlantic hurricanes. *Geophys. Res. Lett.*, 33, L17712,  
344 doi:10.1029/2006GL026267.

345 **Table 1.** The eight strongest (+) phase years within the period 1950-2010 are selected for each  
346 index. Using HURDAT, the number of tropical storms (TS), hurricanes (HR), major hurricanes  
347 (MH, categories 3-5), accumulated cyclone energy (ACE), and number of United States  
348 landfalling hurricanes (USL) are averaged for each index's eight-year composite. For wind shear,  
349 the vertical wind shear (VWS) anomalies in June – November (JJASON) are averaged over the  
350 main development region (MDR, 85°W – 15°W, 10°N – 20°N) for each index's eight-year  
351 composite. The values in parenthesis are those after the influence of MDR SST is removed by  
352 using the method of linear regression. The regression coefficient ( $a = -1.96 \text{ m s}^{-1} \text{ } ^\circ\text{C}^{-1}$ ) is above  
353 99% significance level (see Figure S1). Any value larger or smaller than the climatological mean  
354 with above the 90% significance is in bold.

Index	TS (#)	HR (#)	MH (#)	ACE ( $10^4 \text{ kt}^2$ )	USL(#)	VWS ( $\text{ms}^{-1}$ )
CPW	11 (11)	6 (6)	2 (2)	97.0 (91.3)	2 (2)	0.3 (0.4)
EMI	10 (10)	6 (6)	2 (2)	96.9 (99.9)	2 (2)	0.1 (0.1)
TNI	14 (12)	8 (7)	3 (3)	120.1 (105.9)	2 (2)	-0.3 (0.0)
PMM	11 (11)	7 (7)	3 (3)	103.3 (104.0)	1 (1)	0.2 (0.2)
EPW	<b>8</b> <b>(8)</b>	<b>3</b> <b>(3)</b>	<b>1</b> <b>(1)</b>	<b>53.6</b> <b>(51.7)</b>	<b>1</b> <b>(1)</b>	<b>1.4</b> <b>(1.5)</b>
Climatology	11	7	3	106.3	2	0.0

355

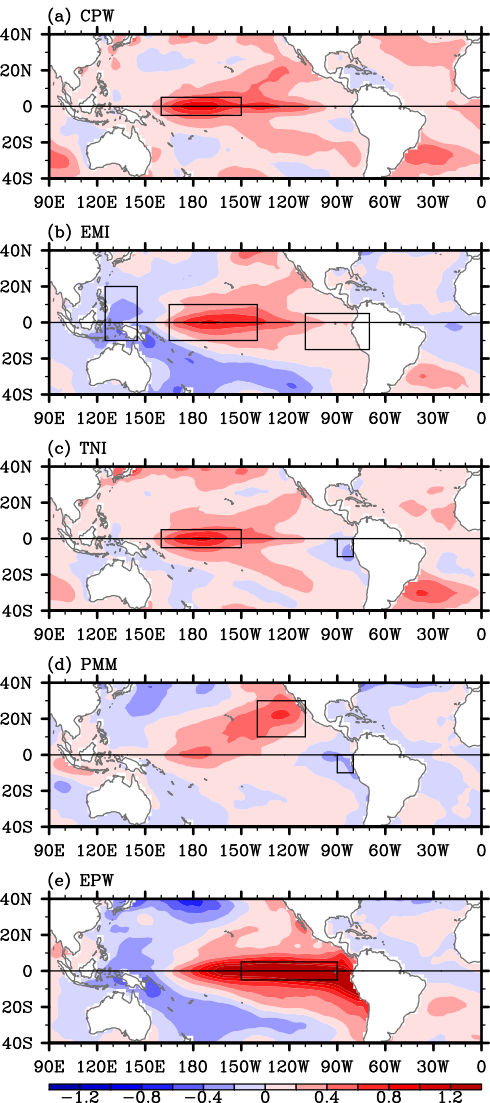
356 **Figure 1.** Composites of SST anomalies in JJASON for the eight strongest (+) phase (a) CPW,  
357 (b) EMI, (c) TNI, (d) PMM and (e) EPW years. The unit is °C. The black boxes indicate the SST  
358 regions referenced for the definitions of (a) CPW (Niño-4), (b) EMI (SSTA(A), SSTA(B), and  
359 SSTA(C)), (c) TNI (Niño-4 and Niño-1+2), (d) PMM (ENP and Niño-1+2) and (e) EPW (Niño-  
360 3). See text for exact definitions of these SST regions.

361

362 **Figure 2.** Composites of geopotential thickness (200 minus 850 hPa) anomalies in JJASON for  
363 the eight strongest (+) phase CPW, EMI, TNI, PMM and EPW years. The influence of MDR  
364 SST is removed prior to making these composites by using the method of linear regression. The  
365 unit is gpm. The black box in each plot indicates the main development region (MDR, 85°W –  
366 15°W, 10°N – 20°N).

367

368 **Figure 3.** Composites of vertical wind shear (200 minus 850 hPa) anomalies in JJASON for the  
369 eight strongest (+) phase CPW, EMI, TNI, PMM and EPW years. The influence of MDR SST is  
370 removed prior to making these composites by using the method of linear regression. The unit is  
371  $\text{m s}^{-1}$ . The black box in each plot indicates the main development region (MDR, 85°W – 15°W,  
372 10°N – 20°N).





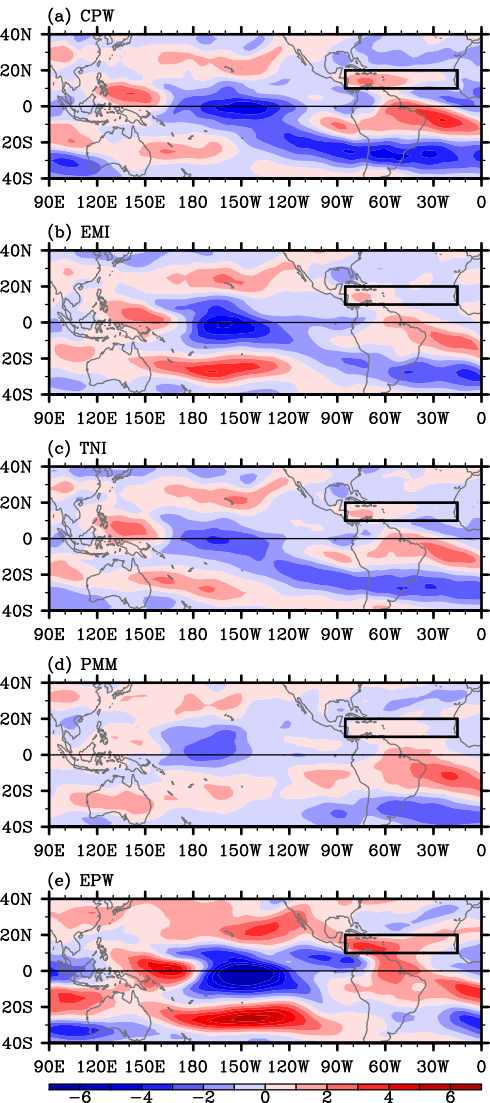


**Table S1.** Correlation coefficients between EMI, TNI, PMM and EPW (NINO3) for JJASON. The values in parenthesis are those for ASO. Correlation coefficients above the 95% significance based on student's t test are in bold.

	EMI	TNI	PMM	EPW
EMI	-	<b>0.86</b> (0.87)	<b>0.53</b> (0.51)	0.17 (0.23)
TNI	<b>0.86</b> (0.87)	-	<b>0.70</b> (0.66)	-0.14 (-0.07)
PMM	<b>0.53</b> (0.51)	<b>0.70</b> (0.66)	-	-0.42 -0.40
EPW	0.17 (0.23)	-0.14 (-0.07)	<b>-0.42</b> (-0.40)	-

**Table S2.** Hurricane indices for the eight strongest CPW years during 1950-2010. The number of tropical storms (TS), hurricanes (HR), major hurricanes (MH, categories 3-5), accumulated cyclone energy (ACE), and number of United States landfalling hurricanes (USL) obtained from HURDAT are shown. For wind shear, the vertical wind shear (VWS) anomalies in JJASON are averaged over the main development region (MDR, 85°W – 15°W, 10°N – 20°N). The values in parenthesis are those after the influence of MDR SST is removed by using the method of linear regression. The regression coefficient ( $a = -1.96 m s^{-1} °C^{-1}$ ) is above 99% significance level (see Figure S1).

Year	NINO4	TS (#)	HR (#)	MH (#)	ACE ( $10^4 kt^2$ )	USL(#)	VWS ( $ms^{-1}$ )
2002	0.96	12 (12)	4 (4)	2 (2)	63.5 (57.1)	1 (1)	1.3 ( 1.4)
1994	0.89	7 (9)	3 (4)	0 (1)	28.8 (50.8)	0 (0)	0.0 (-0.5)
2004	0.88	15 (12)	9 (7)	6 (5)	227.3 (183.9)	6 (6)	-1.0 (-0.1)
2003	0.57	16 (13)	7 (5)	3 (2)	180.3 (143.8)	2 (2)	-0.5 ( 0.3)
1986	0.48	6 (9)	4 (6)	0 (1)	41.4 (75.8)	2 (2)	2.1 ( 1.4)
2001	0.46	15 (13)	9 (8)	4 (3)	115.6 (91.6)	0 (0)	-0.3 ( 0.2)
1990	0.45	14 (13)	8 (7)	1 (1)	93.0 (76.3)	0 (0)	-0.3 ( 0.1)
1977	0.44	6 (8)	5 (6)	1 (2)	26.5 (50.8)	1 (1)	1.0 ( 0.5)
Climatology	0.00	11	7	3	106.3	2	0.0

**Table S3.** Same as Table S2, but for the eight strongest positive EMI years during 1950-2010.

Year	EMI	TS (#)	HR (#)	MH (#)	ACE ( $10^4 kt^2$ )	USL(#)	VWS ( $ms^{-1}$ )
1994	1.50	7 (9)	3 (4)	0 (1)	28.8 (50.8)	0 (0)	0.0 (-0.5)
1966	1.38	11 (11)	7 (7)	3 (3)	148.9 (146.3)	2 (2)	-0.9 (-0.9)
2004	1.24	15 (12)	9 (7)	6 (5)	227.3 (183.9)	6 (6)	-1.0 (-0.1)
1990	1.10	14 (13)	8 (7)	1 (1)	93.0 (76.3)	0 (0)	-0.3 (0.1)
1977	1.05	6 (8)	5 (6)	1 (2)	26.5 (50.8)	1 (1)	1.0 (0.5)
1991	1.04	8 (10)	4 (5)	2 (3)	39.2 (63.6)	1 (1)	1.6 (1.0)
1958	0.75	10 (8)	7 (6)	5 (4)	127.2 (100.1)	1 (1)	-0.3 (-0.3)
1965	0.74	6 (8)	4 (5)	1 (2)	84.3 (111.3)	1 (1)	0.6 (0.1)
Climatology	0.00	11	7	3	106.3	2	0.0

**Table S4.** Same as Table S2, but for the eight strongest positive TNI years during 1950-2010.

Year	TNI	TS (#)	HR (#)	MH (#)	ACE ( $10^4 kt^2$ )	USL(#)	VWS ( $ms^{-1}$ )
1994	1.44	7 (9)	3 (4)	0 (1)	28.8 (50.8)	0 (0)	0.0 (-0.5)
2001	1.33	15 (13)	9 (8)	4 (3)	115.6 (91.6)	0 (0)	-0.3 (0.2)
2004	1.23	15 (12)	9 (7)	6 (5)	227.3 (183.9)	6 (6)	-1.0 (-0.1)
1977	1.09	6 (8)	5 (6)	1 (2)	26.5 (50.8)	1 (1)	1.0 (0.5)
1966	1.04	11 (11)	7 (7)	3 (3)	148.9 (146.3)	2 (2)	-0.9 (-0.9)
2005	1.03	28 (23)	15 (12)	7 (5)	257.5 (189.7)	6 (6)	-2.2 (-0.7)
1990	1.01	14 (13)	8 (7)	1 (1)	93.0 (76.3)	0 (0)	-0.3 (0.1)
2002	0.98	12 (12)	4 (4)	2 (2)	63.5 (57.1)	1 (1)	1.3 (1.4)
Climatology	0.00	11	7	3	106.3	2	0.0

**Table S5.** Same as Table S2, but for the eight strongest positive PMM years during 1950-2010.

Year	PMM	TS (#)	HR (#)	MH (#)	ACE ( $10^4 kt^2$ )	USL(#)	VWS ( $ms^{-1}$ )
1992	1.39	7 (8)	4 (5)	1 (1)	77.3 (92.3)	1 (1)	0.7 (0.3)
1990	1.23	14 (13)	8 (7)	1 (1)	93.0 (76.3)	0 (0)	-0.3 (0.1)
1996	1.12	13 (13)	9 (9)	6 (6)	177.2 (180.0)	2 (2)	0.8 (0.7)
1958	0.94	10 (8)	7 (6)	5 (4)	127.2 (100.1)	1 (1)	-0.3 (-0.3)
2001	0.89	15 (13)	9 (8)	4 (3)	115.6 (91.6)	0 (0)	-0.3 (0.2)
1968	0.72	8 (9)	4 (5)	0 (7)	45.9 (69.7)	1 (1)	-0.2 (-0.8)
1986	0.68	6 (9)	4 (6)	0 (1)	41.4 (75.8)	2 (2)	2.1 (1.4)
1966	0.67	11 (11)	7 (7)	3 (3)	148.9 (146.3)	2 (2)	-0.9 (-0.9)
Climatology	0.00	11	7	3	106.3	2	0.0

**Table S6.** Same as Table S2, but for the eight strongest canonical El Niño (EPW) years during 1950-2010.

Year	NINO3	TS (#)	HR (#)	MH (#)	ACE ( $10^4 kt^2$ )	USL(#)	VWS ( $ms^{-1}$ )
1997	2.78	8 (6)	3 (2)	1 (0)	41.4 (19.6)	1 (1)	0.2 (0.7)
1972	1.71	7 (10)	3 (5)	0 (1)	36.7 (70.0)	1 (1)	3.4 (2.7)
1982	1.67	6 (8)	2 (3)	1 (2)	31.5 (55.5)	0 (0)	2.7 (2.1)
1987	1.41	7 (4)	3 (1)	1 (0)	30.2 (0.0)	1 (1)	1.3 (2.1)
1965	1.21	6 (8)	4 (5)	1 (2)	84.3 (111.3)	1 (1)	0.6 (0.1)
1957	1.08	8 (8)	3 (3)	2 (2)	86.8 (84.9)	1 (1)	-0.2 (-0.2)
2009	0.96	9 (6)	3 (2)	2 (1)	54.6 (22.0)	0 (0)	2.1 (2.8)
1991	0.89	8 (10)	4 (5)	2 (3)	39.2 (63.6)	1 (1)	1.6 (1.1)
Climatology	0.00	11	7	3	106.3	2	0.0

**Table S7.** Same as Table 1, but only for August-October (ASO).

Index	TS (#)	HR (#)	MH (#)	ACE ( $10^4 kt^2$ )	USL(#)	VWS ( $ms^{-1}$ )
CPW	9 (8)	5 (4)	2 (2)	86.5 (75.9)	1 (1)	0.1 (0.4)
EMI	8 (8)	5 (5)	2 (2)	81.9 (81.7)	0 (0)	0.0 (0.0)
TNI	10 (9)	6 (5)	3 (2)	95.4 (82.0)	2 (1)	-0.2 (0.1)
PMM	10 (9)	6 (6)	3 (3)	115.9 (102.1)	1 (1)	-0.2 (0.2)
EPW	<b>6</b> <b>(6)</b>	<b>3</b> <b>(3)</b>	<b>1</b> <b>(1)</b>	<b>50.0</b> <b>(49.4)</b>	<b>0</b> <b>(0)</b>	<b>0.9</b> <b>(0.9)</b>
Climatology	8	5	3	93.3	1	0.0

**Table S8.** Same as Table 1, but by using only the five strongest (+) phase years.

Index	TS (#)	HR (#)	MH (#)	ACE ( $10^4 kt^2$ )	USL(#)	VWS ( $ms^{-1}$ )
CPW	11 (11)	5 (5)	2 (2)	108.5 (102.3)	2 (2)	0.4 (0.5)
EMI	11 (10)	6 (6)	2 (2)	104.9 (101.6)	2 (2)	-0.2 (-0.2)
TNI	11 (10)	7 (6)	3 (3)	109.4 (104.7)	2 (2)	-0.3 (-0.2)
PMM	12 (11)	7 (7)	3 (3)	118.0 (108.1)	1 (1)	0.1 ( <b>0.3</b> )
EPW	<b>7</b> (7)	<b>3</b> (3)	<b>1</b> (1)	<b>44.8</b> ( <b>50.0</b> )	<b>1</b> (1)	<b>1.6</b> ( <b>1.5</b> )
Climatology	8	5	3	93.3	1	0.0

**Table S9.** Same as Table S2, but for the five CPW years considered in Kim et al. [2009] and Lee et al. [2010]. All indices in this table are averaged for August-October (ASO).

Year	NINO4	TS (#)	HR (#)	MH (#)	ACE ( $10^4 kt^2$ )	USL(#)	VWS ( $ms^{-1}$ )
2004	1.00	13 (10)	8 (6)	5 (4)	214.4 (167.7)	5 (5)	-1.2 (0.1)
1994	0.94	4 (6)	1 (2)	0 (1)	10.0 (31.1)	0 (0)	0.0 (-0.6)
2002	0.94	11 (10)	4 (4)	2 (2)	61.0 (49.7)	1 (1)	1.6 (2.0)
1991	0.79	7 (8)	4 (5)	2 (2)	38.0 (53.8)	1 (1)	0.6 (0.1)
1969	0.58	16 (15)	11 (10)	5 (5)	155.9 (143.0)	2 (2)	-0.4 (0.0)
Mean	0.85	10 (10)	6 (5)	3 (3)	95.9 (89.1)	2 (2)	0.1 (0.3)
Climatology	0.00	8	5	3	93.3	1	0.0

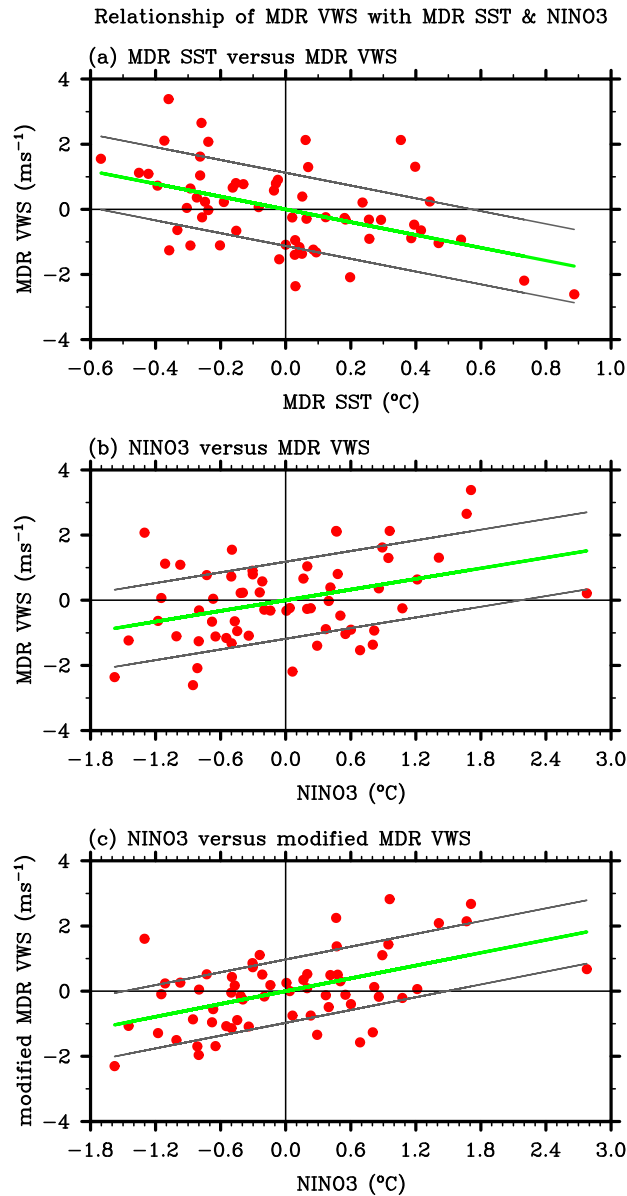


**Figure S1.** Scatterplot of (a) MDR SST versus MDR vertical wind shear (VWS), (b) NINO3 versus MDR VWS, and (c) NINO3 versus modified MDR VWS. All indices are those averaged for JJASON. The influence of MDR SST is removed in the modified MDR VWS by using the method of linear regression. For each plot, the green line is the linear regression, whereas the two gray lines show the standard error of the linear regression. The slope of the regression line is -1.96, 0.55, and 0.65 for (a), (b) and (c), respectively. All three linear regression lines are above the 99% significance level.

## ERSST3: EOF2 (JJASON)

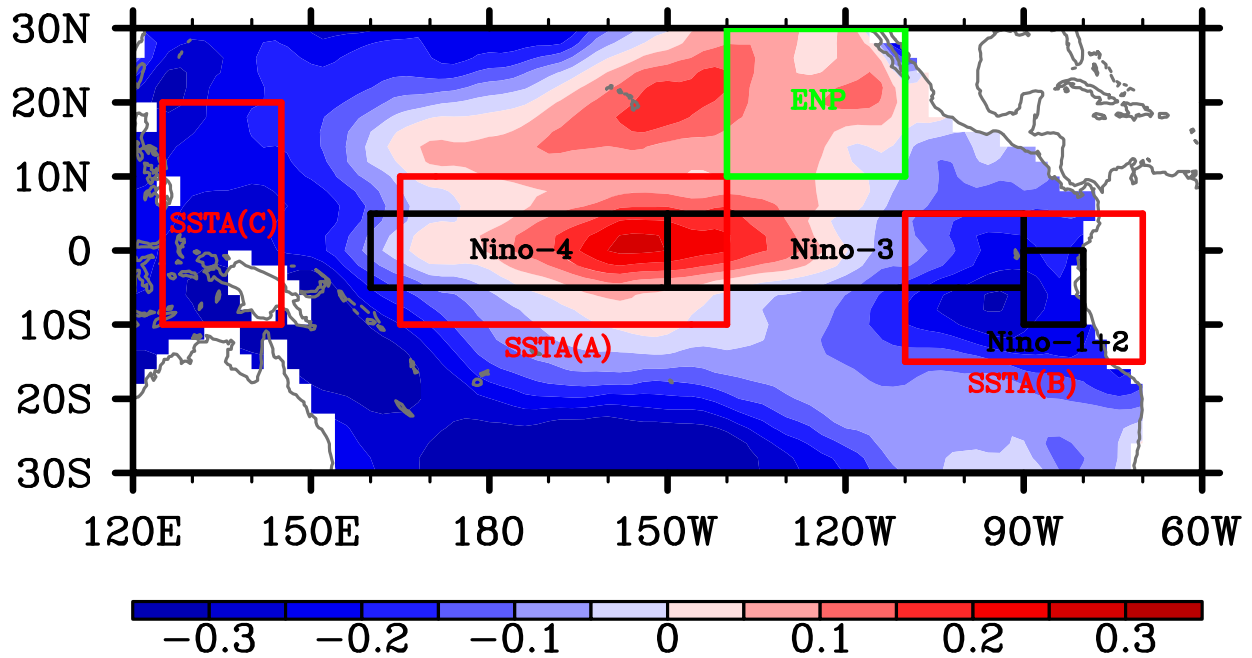


**Figure S2.** SST regions referenced for the definitions of four non-canonical El Niño patterns. See text for exact definitions of these SST regions. The background is the 2nd mode of the empirical orthogonal function (EOF2) analysis of the tropical Pacific SST anomalies. It is constructed by regressing the normalized EOF2 time series onto SST anomalies then averaging the regression coefficients for JJASON.

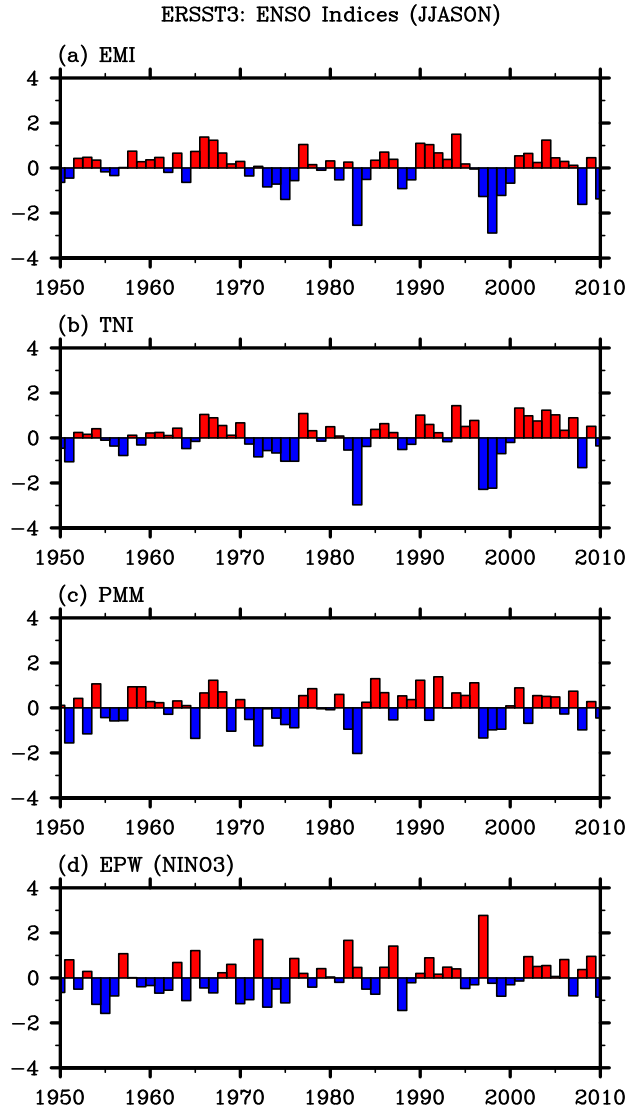


**Figure S3.** Time series of four non-canonical El Niño indices and the canonical El Niño (NINO3) index for JJASON during the period of 1950 - 2010. Each of the four non-canonical El Niño index is normalized by the standard deviation.